

See discussions, stats, and author profiles for this publication at: <https://www.researchgate.net/publication/231409536>

# Chemical and physical properties of electrochemically prepared polyaniline p-toluenesulfonates

ARTICLE *in* THE JOURNAL OF PHYSICAL CHEMISTRY · JUNE 1989

Impact Factor: 2.78 · DOI: 10.1021/j100348a050

---

CITATIONS

5

---

READS

19

3 AUTHORS, INCLUDING:



Kyung M Choi

University of California, Irvine

50 PUBLICATIONS 679 CITATIONS

SEE PROFILE

# The Chemical and Physical Properties of Electrochemically Prepared Polyaniline *p*-Toluenesulfonates

Kyung Moon Choi, Keu Hong Kim,\* and Jae Shi Choi

Department of Chemistry, Yonsei University, Seoul 120, Korea (Received: June 30, 1988)

Polyaniline *p*-toluenesulfonate (PATS) was synthesized by the electrochemical technique from 0.2 M aniline in 1:99 water/acetonitrile solution containing 0.1 M tetraethylammonium *p*-toluenesulfonate (TEATS) as supporting electrolyte. Following the polarographic and cyclic voltammetry measurements, the values of the half-wave potential, transfer coefficient and number of electrons were measured to be 516 mV, 0.49, and 1, respectively. The results of TGA and DSC showed that the weight loss was most rapid in the temperature range from 553 to 653 K, and the maximum value of the reaction rate was 0.23 mg/min at 611 K. The electrical conductivity of PATS was measured in the temperature range from 123 to 298 K. From the plot of resistivity vs  $1/T$ ,  $E_a$  was obtained to be 0.038 eV. From the temperature dependence of the conductivity and ESR measurements, it is suggested that the conduction mechanism for PATS is possibly a small polaron hopping conduction.

## Introduction

Various conducting polymers have been reported on in many papers<sup>1-5</sup> during recent years. These materials have generated widespread interest as potential choice materials for a variety of applications in different areas including solar energy conversion, batteries, electronics, and corrosion.

The early studies on these polymers were mainly performed with conjugated organic polymers prepared by chemical synthesis. Then, their conductivities could be increased by doping with various donors or acceptors. Chiang et al.<sup>6</sup> reported that the electrical conductivity of  $(CH)_x$  doped with halogen could be systematically increased by more than 8 orders of magnitude. The associated  $E_a$  decreased from an initial value of about 0.3–0.01 eV. The maximum room temperature conductivity for iodine dopant exceeded 500 (ohm-cm)<sup>-1</sup>.

However, recently, the attraction of electrochemically polymerized conducting polymers has prompted us to study these electroactive materials. In previous studies, polypyrrole derivatives<sup>3,4</sup> have been mainly investigated. Conducting polypyrrole film, available via the electrochemical oxidation of pyrrole, has often been reported as the electrode material.<sup>7,8</sup> Thin films of polypyrrole are electroactive and electrochromic<sup>7</sup> and have been considered for ion gate applications and displays.<sup>8</sup>

Pfluger et al.<sup>9</sup> have reported numerous studies for pyrrole-based conducting polymers. They obtained free-standing films of insulating neutral polypyrrole (PP<sup>0</sup>) prepared by electrochemical reduction of PP<sup>+</sup> under drybox conditions.<sup>10</sup> Thus, spectroscopic, conductivity, and weight uptake data were used to characterize the nature of the conversion of PP<sup>0</sup> to PP<sup>+</sup>. It has been suggested that the oxidation of PP<sup>0</sup> occurs by homogeneous charge extraction from the  $\pi$ -system of the unaffected polypyrrole.

Diaz et al.<sup>2</sup> published an attempt to explain the electropolymerization mechanism of pyrrole in acetonitrile solution containing BF<sub>4</sub><sup>-</sup> anions. They concluded that polymerization should take place through a previously produced pyrrole  $\pi$ -radical cation,

formed by one electron transfer, which would act as the monomer for polymerization by reaction with neighboring pyrrole molecules. On the other hand, Prejza et al.<sup>11</sup> reported that the BF<sub>4</sub><sup>-</sup> could play a role in the initiation step of polymerization. The oxidation of this substance takes place at a higher cathodic potential than is necessary for the oxidation of the monomer. The oxidation of the polymeric form of the pyrrole would give rise to the conducting state of the polypyrrole layer.

Polyaniline is one of the conducting polymers in which the transition between the insulating and conducting states may involve only migration of a proton through the film solution interface to maintain charge neutrality. Also, unlike most conducting polymers, polyaniline is readily prepared from aqueous solution and the conducting form is stable in air and water. Through numerous studies, the applicability of polyaniline in batteries,<sup>12</sup> microelectronic devices,<sup>13</sup> ion exchanges,<sup>14</sup> and electrochromic displays<sup>15</sup> has been demonstrated.

Jozefowicz et al.<sup>16</sup> reported that a pressed pellet of polyaniline, when it was placed between a mercury electrode and aqueous H<sub>2</sub>SO<sub>4</sub>, produced an open circuit potential which decreased as the pH of the solution increased. This result implies that the sample in this arrangement has both ionic and electronic conductivities. Also, MacDiarmid et al.<sup>5</sup> have sought to obtain a more complete understanding of the oxidation/reduction relationship of polyaniline. In these studies, cyclic voltammetry showed an excellent reversibility between reduced and oxidized forms of polyaniline; and the Coulombic capacity decreased only to 99.1% after the 50th cycle. These observations are important in battery studies.

However, polyaniline doped with various anions via electrochemical methods has not been investigated extensively. Thus, in this work, we will present the results of a mechanistic study of polyaniline doped with *p*-toluenesulfonate via an electrochemical reaction and elucidate on the morphology, thermal stability, magnetic property, and electrical conduction mechanism.

## Experimental Section

**Materials.** Tetraethylammonium *p*-toluenesulfonate (TEATS) as a supporting electrolyte was obtained from the Aldrich Chemical Co. Owing to the hygroscopic nature of TEATS, it was dried under vacuum at 25 °C for 2 days. Aniline was purified by vacuum distillation.

(1) Shacklette, L. W.; Elsenbaumer, R. L.; Chance, R. R.; Eckhardt, H.; Frommer, J. E.; Baughman, R. H. *J. Chem. Phys.* **1981**, *75*(4), 1919.

(2) Diaz, A. F.; Kanazawa, K. K. *Extended Linear Chain Compounds*; Miller, J., Ed.; Plenum Press: New York, 1982; Vol. 3, p 417.

(3) Prejza, J.; Lundstrom, I.; Skotheim, T. J. *Electrochem. Soc.* **1982**, *129*, 1685.

(4) Diaz, A. F.; Hall, B. *IBM J. Res. Dev.* **1983**, *27*(4), 342.

(5) MacDiarmid, A. G.; Chiang, J. C.; Huang, W.; Humphrey, B. D.; Somasiri, N. L. D. *Mol. Cryst. Liq. Cryst.* **1985**, *125*, 300.

(6) Chiang, C. K.; Park, Y. W.; Heeger, A. J. *J. Chem. Phys.* **1978**, *69*(11), 1.

(7) Diaz, A. F.; Castillo, J. I.; Logan, J. A.; Lee, W. Y. *J. Electroanal. Chem.* **1981**, *129*, 115.

(8) Burgmayer, P.; Murray, R. W. *J. Am. Chem. Soc.* **1982**, *104*, 6139.

(9) Pfluger, P.; Krounbi, M.; Street, G. B. *J. Chem. Phys.* **1983**, *78*(6), 3212.

(10) Street, G. B.; Clarke, T. C.; Krounbi, M.; Kanazawa, K. K.; Lee, V.; Pfluger, P.; Scott, J. C.; Weiser, G. *Mol. Cryst. Liq. Cryst.* **1982**, *83*, 1285.

(11) Prejza, J.; Lundstrom, I.; Skotheim, T. J. *Electrochem. Soc.* **1982**, *129*, 1685.

(12) Kitani, A.; Kaya, M.; Sasaki, K. *J. Electrochem. Soc.* **1986**, *133*, 1069.

(13) Paul, E. W.; Rizzo, A. J.; Wrighton, M. S. *J. Phys. Chem.* **1985**, *89*, 1441.

(14) Oyama, N.; Ohsaka, T.; Shimizu, T. *Anal. Chem.* **1985**, *57*, 1526.

(15) Gottesfeld, S.; Redondo, A.; Feldberg, S. W. *J. Electrochem. Soc.* **1987**, *134*, 271.

(16) Jozefowicz, M.; Yu, L. T.; Perichon, J.; Buvet, R. *J. Polym. Sci., C* **1969**, *22*, 1187.

TABLE I: Results of Elemental Analysis for PATS<sup>a</sup>

polymer			anion			
C	H	N	C	H	S	O
5.60	5.31	1.00	3.57	3.57	0.50	1.90

<sup>a</sup> Each value is given as an atom mole ratio normalized to nitrogen.

Acetonitrile (AN), most widely used as an organic solvent for anodic electrochemistry at present, was also prepared as a solvent. In order to support the passage of an electrical current, the solvent system should have a low electrical resistance and a moderately high dielectric constant, since the prevalence of ion pairing and even multiple ionic associations in less polar solvents results in low ionic mobility and conductance in such solutions. For the removal of water and acrylonitrile, the main impurities in acetonitrile, the solvent was passed through a column packed with alumina previously dried at 400 °C.

**Sample Preparation.** Polyaniline *p*-toluenesulfonate (PATS) was prepared from 0.2 M aniline in 1:99 (volume %) water/ acetonitrile solution containing 0.1 M tetraethylammonium *p*-toluenesulfonate (TEATS) as a supporting electrolyte. This solution was deoxygenated by stirring it with a nitrogen stream for 30 min before every experiment. Using a Lauda Circulator, the temperature of the system was maintained at 25 °C.

The three-electrode cell was equipped with a Pt working electrode, a Pt counter electrode, and a standard calomel electrode. The working electrode was a 2-cm<sup>2</sup> Pt plate, and a 1-cm<sup>2</sup> Pt cylinder was used as the counter electrode.

PATS was electrochemically synthesized in the potential range between 1.5 and 1.8 V vs SCE. The anodic insoluble precipitates produced from the reaction remained on the electrode and were confirmed to be the electrically conductive polymers.

The rate of material growth depended directly on the current density; in other words, there was a linear dependence on time. The current density varied with the resistance of the electrolytic solution, the concentration of the aniline, and the applied voltage.

The synthesis time was controlled to between 1 and 7 h, resulting in adhering materials of adequate thickness for various experimental purposes. This product was removed from the anodic electrode, rinsed with acetonitrile, and dried in a vacuum oven for 2 days. Elemental analysis was performed to determine the dopant content in the final product. This result is shown in Table I.

**Electrochemical Measurements.** Electrochemical measurements were performed by using a Tacussel potentiostat (Polaropulse Type PRG-5), with potential sweeps applied from a Tacussel function generator (Model No. GSTP 3). The voltammograms were plotted using a Rikadenki X-Y recorder.

**Conductivity Measurements.** Electrical conductivity was measured by the four-probe technique at temperatures from 123 to 298 K. The current and the voltage were measured by a Keithley 616 digital electrometer and a 642 digital multimeter, respectively. Before the experiments, the specimen was heat-treated at a temperature near the melting point to remove residual trapped carriers or dipole orientation effects.

The sample was placed in a temperature-controlled chamber and the required temperature obtained by using liquid nitrogen. The conductivity was measured while raising the temperature at a heating rate of 1 °C/min. The conductivity values were calculated directly from the measured resistance and sample dimensions.

**ESR Measurements.** Electron spin resonance (ESR) measurements were performed with a Bruker EPR spectrometer (Model No. ER 200 E-SRC). Polyaniline *p*-toluenesulfonate (PATS) powders were placed in the ESR tube and ESR measurements carried out under the following conditions: scan range, 50 G; time constant, 200 s; modulation amplitude, 0.4 G; field set, 3360 G; receiver gain, 125; microwave power, 20 mW; modulation frequency, 100 kHz; microwave frequency, 9.45 GHz; temperature, 25 °C.

**Thermal Analysis.** The thermal gravimetric analysis (TGA) and differential scanning calorimetry (DSC) measurements were

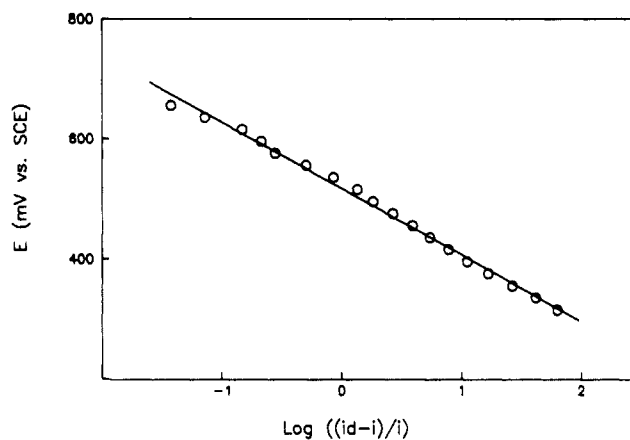


Figure 1. Plot of  $E$  vs  $\log ((i_d - i)/i)$  for 0.2 M aniline in 1:99 water/AN solution containing 0.1 M TEATS at 25 °C.

performed with a thermal analyzer (Rigaku, Model No. 8150). TGA analysis under a nitrogen atmosphere was carried out at temperatures in the range of 273–1073 K with a heating rate of 10 °C/min.

**Scanning Electron Microscopy (SEM).** SEM was performed by using a scanning electron microscope (Hitachi, Model No. S-510) and ion coater (Eiko, Model No. IB-3).

## Results and Discussion

**Polarography.** A polarogram of the 0.2 M aniline in 1:99 water/acetonitrile solution containing 0.1 M TEATS was obtained at 25 °C. The magnitude of the diffusion-controlled currents is a direct function of depolarizer concentration, making quantitative analysis by polarography possible. All quantitative analysis by this technique is based on the direct proportionality between the diffusion-controlled limiting current and the depolarizer concentration.

In the reversible reactions, the relationship between the potential of a dropping mercury electrode (vs reference electrode) and the diffusion current is shown by the Heyrovsky–Ilkovic<sup>17</sup> equation

$$E = E_{1/2} + (2.303RT/nF) \log ((i_d - i)/i) \quad (1)$$

where  $i_d$  is the limiting current and  $n$  is the number of electrons exchanged in the electrode reaction. The potential at the midpoint of the wave where  $i = i_d/2$  is known as the half-wave potential,  $E_{1/2}$ , and this quantity is characteristic of a given depolarizer for fixed solution and environmental conditions. The half-wave potential may be used to identify qualitatively the components in a depolarizer mixture. Also, the value of  $E_{1/2}$  is very sensitive to the presence of different complexing species, including supporting electrolyte anions. Therefore, a plot of  $\log ((i_d - i)/i)$  vs  $E$  may be used to determine both  $n$  and an accurate value of  $E_{1/2}$ .

In the case of irreversible reactions, the wave has less than the theoretical slope for the number of electrons transferred and eq 1 must be modified to include  $\alpha$  as a transfer coefficient. Thus, in the irreversible system, we can compute the value of  $\alpha n$  using the following equation

$$E = E_{1/2} + (2.303RT/\alpha nF) \log ((i_d - i)/i) \quad (2)$$

The potential vs SCE is plotted against  $\log ((i_d - i)/i)$  values in Figure 1. The half-wave potential ( $E_{1/2}$ ) obtained from Figure 1 is 516 mV and the value of  $\alpha n$  calculated from the slope of Figure 1 is 0.49.

This value of  $\alpha$  shows a symmetry of the energy barrier. In most systems, the magnitude of  $\alpha$  turns out to lie between 0.3 and 0.7, and it can usually be approximated by 0.5 in the absence of actual measurements. If we assume that the number of electrons transferred in this electrode reaction is one, then the value of  $\alpha$  is 0.49. To provide supporting evidence for this prediction, measurements of cyclic voltammetry were carried out.

(17) Bard, A. J.; Faulkner, L. R. *Electrochemical Methods*; Wiley: New York, 1980.

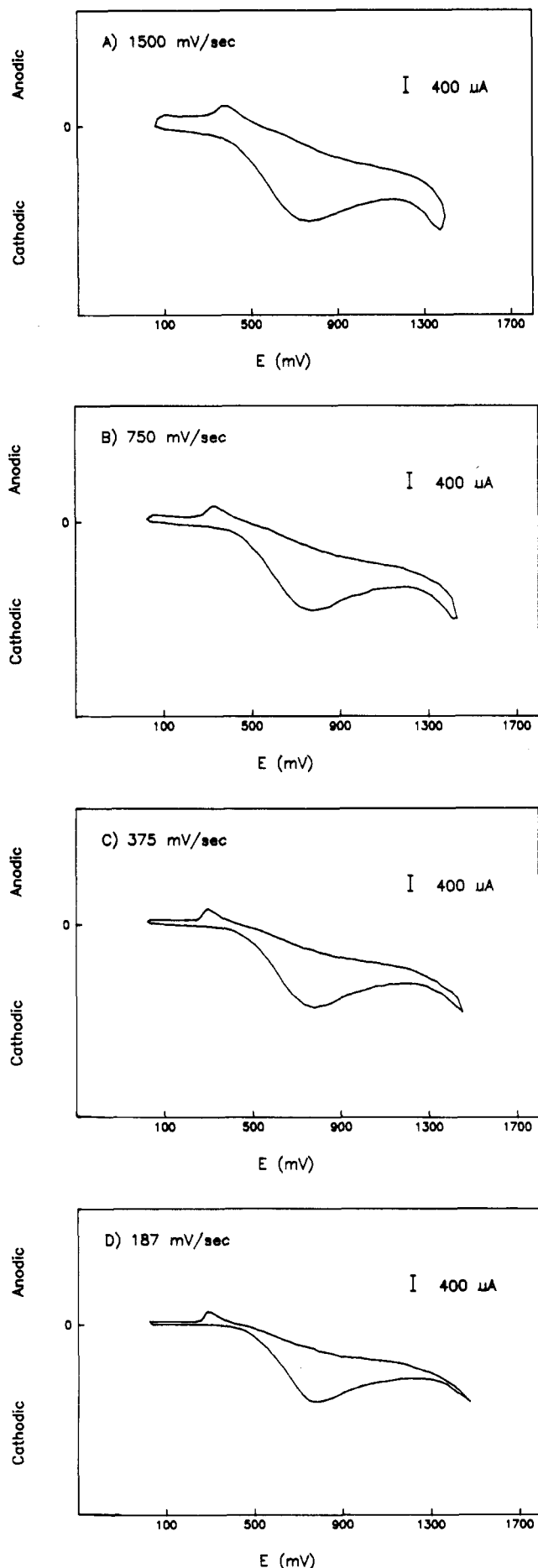


Figure 2. Cyclic voltammogram of a polyaniline *p*-toluenesulfonate film on a Pt electrode in 1:99 water/AN solution at 25 °C.

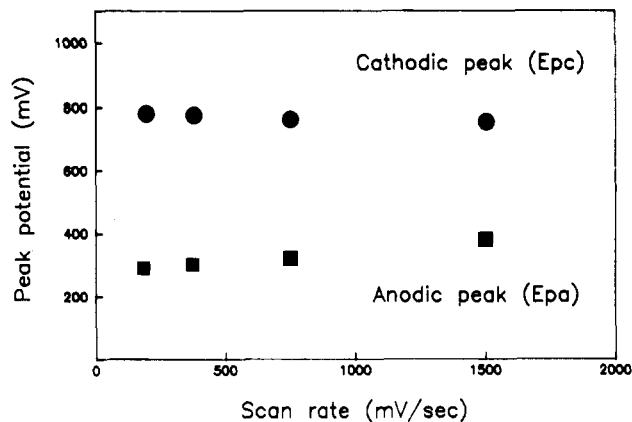


Figure 3. Variations of anodic and cathodic peak potential with scan rate for 0.2 M aniline in 1:99 water/AN solution containing 0.1 M TEATS at 25 °C.

**Cyclic Voltammetry.** Cyclic voltammetry describes a process in which the potential is scanned back and forth between the two limits. The method in its modern form owes much to the efforts of Shain and Nicholson.<sup>18</sup>

The cyclic voltammograms in Figure 2 were obtained from 0.2 M aniline in 1:99 water/acetonitrile solution containing 0.1 M TEATS at 25 °C. The three-electrode cell was equipped with a Pt plate working electrode, a Pt cylindrical counter electrode, and a standard calomel electrode (SCE). After deoxygenation of this solution by a stream of nitrogen, the potential was scanned in the range of 0–1500 mV with various scan rates. Figure 2 shows that the number of electrons transferred in this electrode reaction is one. Thus, it is convinced from a comparison of the polarographic results that the value of  $n$  is 1 and  $\alpha$  is 0.49.

On the other hand, the descending part of the curve follows a  $1/t^{1/2}$  dependence, the current has a shorter time to decrease for fast scans, and the curves decay less in the faster scans. The peak height changes in proportion to the square root of the scan rate,  $V$ , as well as to the concentration of the active species.

For potential sweep experiments, since the potential is continuously changing, the charging current ( $i_c$ ) can be expressed by the following equation

$$|i_c| = AC_dV \quad (3)$$

where  $C_d$  is the electrode capacitance per unit area,  $A$  is the area of the electrode, and  $V$  is the scan rate, and the faradaic current can be measured from the base line of the charging current.

The ratio of  $i_p$  to  $i_c$  is considerable; that is, the peak current ( $i_p$ ) varies with  $V^{1/2}$ , and  $i_c$  varies with  $V$ . Then,  $i_c$  becomes relatively more important at faster scan rates.

$$\frac{|i_c|}{i_p} = \frac{C_d V^{1/2} (10^{-5})}{2.69 n^{3/2} D_0^{1/2} C_0^*} \quad (4)$$

At high  $V$  and low  $C_0^*$  values, severe distortion of the wave occurs. The variations of the anodic and cathodic peak potential ( $E_{pa}$ ,  $E_{pc}$ ) with increasing the scan rate are shown in Figure 3.

**TGA and DSC.** Thermal analysis gives useful information on properties of polymers measured as a function of temperature. TGA is a dynamic method in which the weight loss of a sample is measured continuously as the temperature is changed at a constant rate.

In Figure 4, the TGA curve for PATS under a nitrogen atmosphere shows the weight loss beginning at about 280 °C and increasing to 30% at 380 °C. The corresponding differential scanning calorimetric (DSC) curve shows that no phase transition occurs in the measured temperature range.

The reaction rate ( $dW/dt$ ) is plotted against the reciprocal of absolute temperature in Figure 5. As mentioned above, Figure 5 shows clearly that the weight loss is most rapid in the temperature range from 553 to 653 K. The maximum value of the

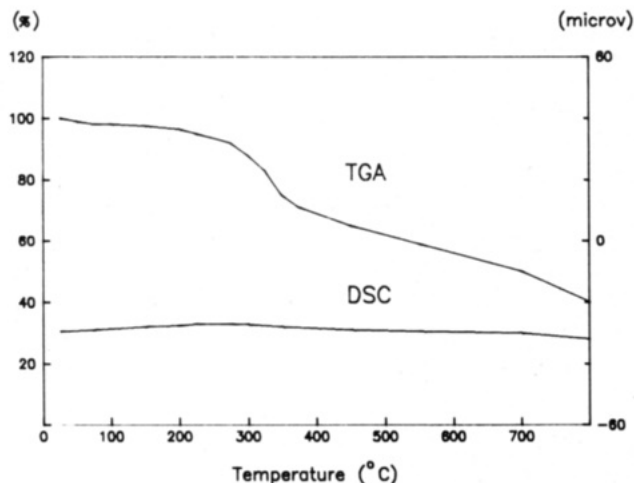


Figure 4. TGA and DSC curves of a polyaniline *p*-toluenesulfonate in nitrogen.

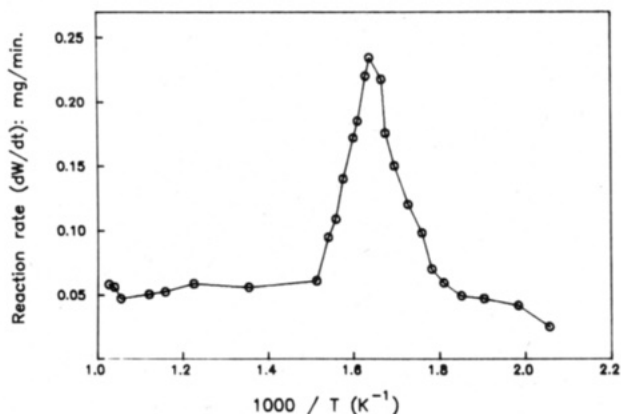


Figure 5. Temperature dependence of the reaction rate for a polyaniline *p*-toluenesulfonate.

reaction rate is 0.23 mg/min at 611 K.

**SEM.** The morphology of the polymer depends mainly on the structure of the monomer, the nature of the dopant, and the thickness of the film grown on the electrode. PATS thin film was grown on anodic Pt electrode from 0.2 M aniline in 1:99 water/AN solution containing 0.1 M TEATS for SEM analysis, using a potential range between 1.5 and 1.8 V vs SCE.

As the reaction progressed, the color of the thin film gradually changed from dark green to black, and the homogeneity of the film surfaces changed from homogeneous to heterogeneous. When the thickness of the PATS film was adequate for SEM analysis, the film was rinsed with acetonitrile.

The most popular thin-film technique for SEM is the sputter coating method. The morphology of the PATS film on Pt is shown in Figure 6. The structure of the PATS film in Figure 6 is rougher than that from previously reported micrographs of polyaniline films.<sup>19</sup> This roughness of PATS film is explained by the doping effect of the *p*-toluenesulfonate anions.

**Conductivity.** In previous studies,<sup>20-24</sup> investigators have suggested equations relevant to specific composites and various models for electrical conduction in composites. However, the precise conducting mechanisms in polymeric systems are not fully understood, since they are influenced by factors such as the dopant level, the morphology of the polymers, orientation of the conducting species, temperature, density, shape, and applied voltage. No band structure may exist in polymers since they have an amorphous matrix. Also, the crystalline-amorphous phase

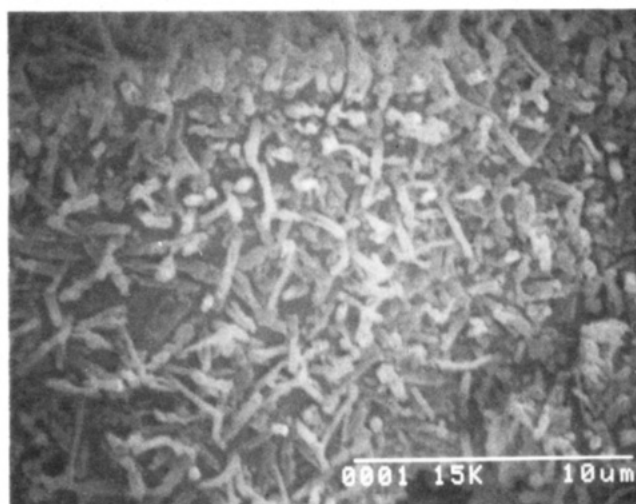
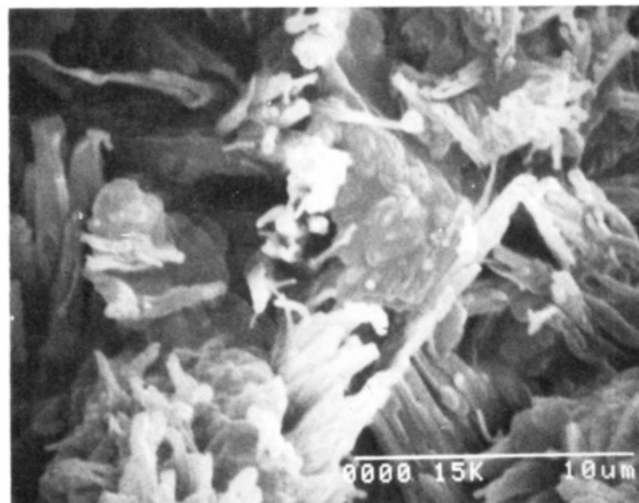


Figure 6. Scanning electron micrograph of a polyaniline *p*-toluenesulfonate film.

boundaries in polymers may lead to large deviation from ideal behavior.

The electrical conductivity as a function of temperature based on the hopping conduction mechanism has been given by Mott<sup>20</sup> and Greaves.<sup>21</sup> Mott's equation is based on a model in which charge is transported by the thermally assisted hopping of electrons through localized states near the randomly distributed "traps"—potential fluctuations that can bind electrons. This equation can be applied in the temperature range from 60 to 300 K. However, this equation is based on the assumption that the concentration of charge carriers has nothing to do with the temperature. According to Greaves,<sup>21</sup> variable range hopping conduction is represented by

$$\sigma T^{1/2} = \exp(-B/T^{1/4}) \quad (5)$$

where  $B$  is a constant. On the other hand, the electrical conductivity as a function of temperature is given by Matare's equation<sup>22</sup>

$$\sigma = AT^{1/2} \exp(-E_a/kT) \quad (6)$$

where  $A$  is a constant and  $E_a$  is the height of the potential barrier. This equation has been derived for a system including grain boundary barriers. Also, Zeller<sup>23</sup> and Orton<sup>24</sup> have shown that tunneling and thermionic emission conduction can be expressed by the following two equations, respectively,

$$\sigma = \sigma_0 \exp(-A/T^{1/2}) \quad (7)$$

$$\sigma = \sigma_0 T^{-1/2} \exp(-E_a/kT) \quad (8)$$

Using a constant potential supply, we obtained enough anodic precipitate to make a pellet. The anodic precipitate was removed

- (19) Diaz, A. F.; Logan, J. A. *J. Electroanal. Chem.* **1980**, *111*, 111.  
 (20) Mott, N. F. *J. Non-Cryst. Solids* **1968**, *1*, 1.  
 (21) Greaves, G. N. *J. Non-Cryst. Solids* **1973**, *11*, 427.  
 (22) Matare, M. F. *J. Appl. Phys.* **1984**, *56*, 2605.  
 (23) Zeller, H. R. *Phys. Rev. Lett.* **1972**, *28*, 1452.  
 (24) Orton, J. W.; Powell, M. J. *Rep. Prog. Phys.* **1980**, *43*, 1263.

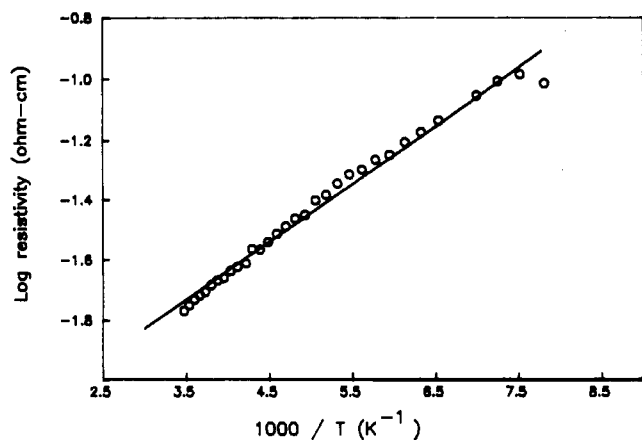


Figure 7. Temperature dependence of the electrical resistivity for a polyaniline *p*-toluenesulfonate.

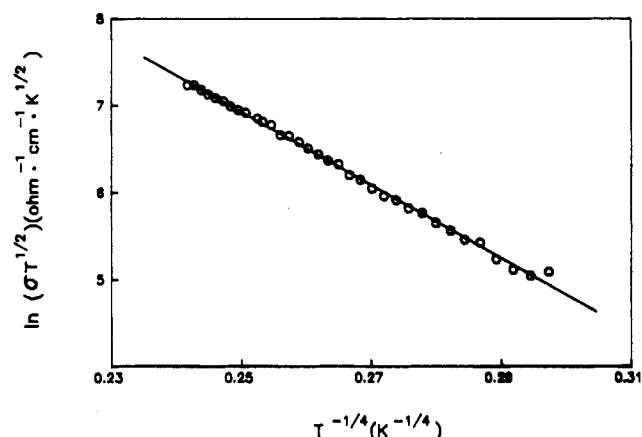


Figure 8. Temperature dependence of the electrical conductivity for a polyaniline *p*-toluenesulfonate, according to the hopping conduction mechanism.

TABLE II: Comparison of Activation Energy and Conductivity at 25 °C for Various Conducting Polymers

conducting polymers	anion doped		anion undoped	
	conductivity, (ohm-cm) <sup>-1</sup>	<i>E<sub>a</sub></i> , eV	conductivity, (ohm-cm) <sup>-1</sup>	<i>E<sub>a</sub></i> , eV
electrochem polythiophene	106.00	0.023	2 × 10 <sup>-8</sup>	0.36
chem polythiophene	0.02	0.085	10 <sup>-14</sup> –10 <sup>-11</sup>	0.98
electrochem PMeT <sup>a</sup>	120.00	0.011		
chem PMeT	0.40	0.062	10 <sup>-14</sup> –10 <sup>-11</sup>	0.98
electrochem PATS	83.00	0.038	10 <sup>-11</sup> –5	

<sup>a</sup> PMeT = poly(3-methylthiophene).

from the electrode, rinsed with acetonitrile, dried under vacuum, and made into a pellet under a pressure of 0.8 tons/cm<sup>2</sup>. The specimen was disk-shaped, 13 mm in diameter, and 1.9 mm thick. The average density of the sample obtained with a pycnometer was 12.85 g/cm<sup>3</sup>.

The measurements of electrical conductivity were performed by a four-probe technique at temperatures from 123 to 298 K under a low applied field to ensure ohmic behavior. The temperature dependence of the resistivity of the pressed pellet of PATS is shown in Figure 7. As shown in Figure 7, the resistivity decreases linearly with increasing temperature, satisfying the Arrhenius equation,  $\rho = \rho_0 \exp(-E_a/kT)$ .  $E_a$  was obtained from the slope of the straight line in Figure 7 and was 0.038 eV. And value of  $\log \sigma$  at 25 °C was evaluated to be 1.9 (ohm-cm)<sup>-1</sup>. Numerous results have been reported for electrochemically and chemically generated conducting polymers. The activation energies and conductivities at 25 °C for various conducting polymers are shown in Table II.

The temperature dependencies of the electrical conductivity of PATS, according to eq 5–8 for the hopping, grain boundary, tunneling, and thermionic emission conduction, are shown in

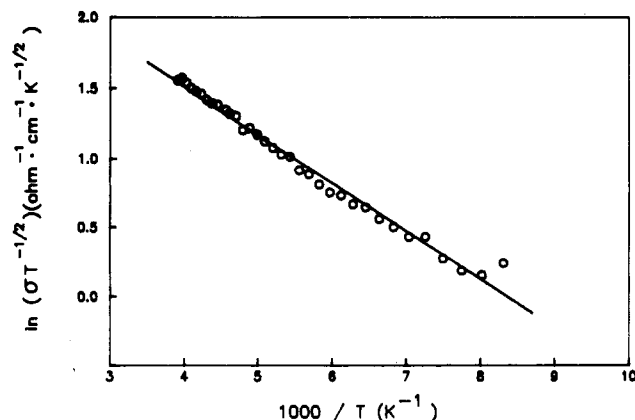


Figure 9. Temperature dependence of the electrical conductivity for a polyaniline *p*-toluenesulfonate, according to  $\sigma = AT^{1/2} \exp(-E_a/kT)$ .

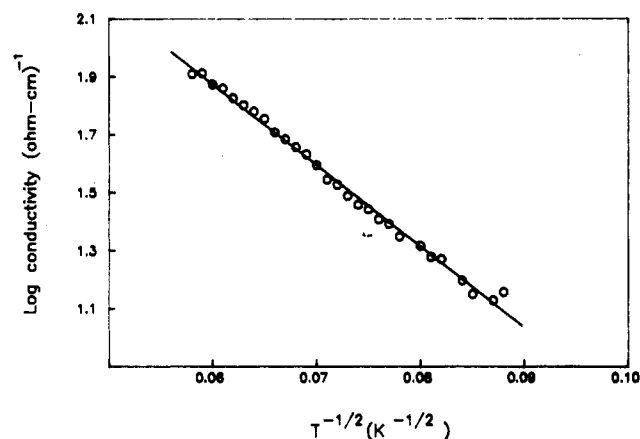


Figure 10. Temperature dependence of the electrical conductivity for a polyaniline *p*-toluenesulfonate, according to the tunneling conduction mechanism.

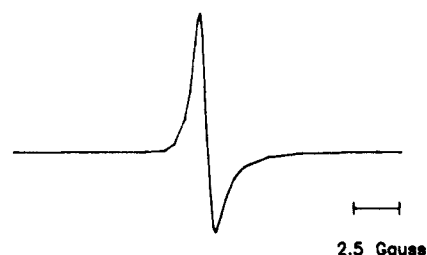


Figure 11. ESR spectrum of a polyaniline *p*-toluenesulfonate at 25 °C (microwave frequency 9.45 GHz).

Figures 8–10, respectively. Then, a plot according to eq 8 was excluded as a poor linearity. Comparing Figure 8 with Figures 9 and 10, the plot of  $\ln \sigma T^{1/2}$  vs  $T^{-1/4}$  shows more linearity than those of  $\ln \sigma T^{1/2}$  vs  $1000/T$  and  $\log \sigma$  vs  $T^{-1/2}$ . That is, the conduction of PATS is predominately carried out by hopping. According to the previous reports, it is predicted that acceptor is formed along the polymer chain in PATS by doping of anions as an electron acceptor, and charge carriers are polaron. It is suggested that the electrical conduction mechanism of PATS is a small polaron hopping mechanism. For evidence of the formation of solitons, singly charged paramagnetic centers, ESR measurements were attempted.

**ESR Measurements.** Recently, a number of ESR studies<sup>25</sup> of conducting polymers have been performed to verify the suggested conduction mechanisms and obtain evidence of the paramagnetic center, the soliton. In previous ESR studies,<sup>16</sup> it was shown that the peak-to-peak line width ( $\Delta H_{pp}$ ) and the  $A/B$  ratio for ESR spectrum of conducting polymer are related to the conductivity.

(25) Chung, T. C.; Feldblum, A.; Heeger, A. J.; MacDiarmid, A. G. *J. Chem. Phys.* **1981**, *74*(10), 5504.

**TABLE III: Comparison of ESR Parameters with Conductivity at 25 °C for Various Polyaniline Derivatives**

polyaniline derivatives	A/B ratio	$\Delta H_{pp}$ , G	g value	log conductivity, (ohm-cm) <sup>-1</sup>
PAP	1.134	90.00	2.001 04	3.111
PATFB	1.714	19.50	2.004 65	2.666
PATS	1.753	0.75	2.004 75	1.919

In Figure 11, the ESR spectrum of the PATS sample at room temperature shows a single peak like that of other conjugated conducting polymers. The measured peak-to-peak line width, A/B ratio, and g value are 0.75 G, 1.7533, and 2.004 75, respectively.

For comparison of the ESR parameters and conductivity for other polyaniline derivatives, polyaniline tetrafluoroborate (PATFB) and polyaniline perchlorate (PAP) were synthesized by the electrochemical and chemical oxidation of aniline, respectively. For these synthesized polyaniline derivatives, the ESR and conductivity measurements were performed by the same methods as in the case of PATS. The values of the ESR parameters and conductivity at 25 °C are summarized in Table III.

Table III shows that the conductivities of various polyaniline derivatives increase with increasing  $\Delta H_{pp}$  and decreasing A/B ratio and decreasing g value.

### Conclusions

The polarography and cyclic voltammetry results show that the oxidation reaction of aniline containing *p*-toluenesulfonate anions

at the anodic electrode is an irreversible reaction relating one electron. In other words, polymerization should take place through a previous production of an aniline  $\pi$ -radical cation, formed by one electron transfer, which would act as the monomer for polymerization by reaction with neighboring aniline molecules. Then, the *p*-toluenesulfonate anion could play a role in the initiation of polymerization.

From the temperature dependence of the electrical conductivity,  $E_a$  is obtained to be 0.038 eV, and the hopping conduction model is suggested. As the ESR measurements show the presence of singly charged paramagnetic centers, the conduction mechanism for PATS is suggested the small polaron hopping conduction. That is, following doping of anions as an electron acceptor, a polaron with 0.038 eV gap is formed near the conduction band. The electron in the level causes a local polarization near the positively charged center, and hence the electron becomes a small polaron with  $\pi$ -cation radical. The observed conduction is due to polarons, charge carriers, that hop from state to state.

**Acknowledgment.** We are grateful to the Ministry of Education of Korea for financial support and to Professor J. W. Park for assistance with the electrochemical measurements. We also thank Professor H. S. So for ESR measurements.

**Registry No.** TEATS, 733-44-8; polyaniline, 25233-30-1; *p*-toluenesulfonate, 16722-51-3; aniline, 62-53-3; tetrafluoroborate, 14874-70-5; perchlorate, 14797-73-0; polythiophene, 25233-34-5; poly(3-methylthiophene), 84928-92-7.

## Electrostatics of Ion-Ion Interactions in Solution

Alexander A. Rashin

Department of Physiology and Biophysics, Mount Sinai School of Medicine of the City University of New York, New York, New York 10029 (Received: September 6, 1988; In Final Form: January 9, 1989)

Potentials of mean force (PMF) between ions in solution are calculated with a method based on a continuum representation of the solvent, and employing the boundary element technique. PMFs calculated with this method for  $\text{Li}^+\text{Cl}^-$ ,  $\text{Na}^+\text{Cl}^-$ , and  $\text{K}^+\text{Cl}^-$  are in quantitative agreement with corresponding PMFs from microscopic theories. The agreement suggests that the double minimum shape of PMF is due to the fact that the energy of unscreened Coulombic interaction and the energy of hydration have different dependence on ion-ion distance. It also suggests that contributions from dielectric saturation, a specific structure of solvent around ions, and nonelectrostatic effects—which were not included in our calculations—are not dominant for PMFs. Differences in details of PMF for like charged ions calculated with macroscopic and microscopic methods can be attributed to the errors involved in calculations of large hydration energies of double-charged systems, or to a slight shrinking of the cavity containing the double charge. It is shown that the larger association constant for an ion pair in a nonassociated solvent than in an associated solvent with the same dielectric constant can be due to larger cavity radii in nonassociated solvents.

### I. Introduction

Many chemical and biochemical phenomena take place in solution, making the evaluation of solvent effects a critical element for understanding these phenomena.<sup>1,2</sup> Ion-ion interactions constitute a particular class of such phenomena crucial for chemical reactions in solution and for the structure and function of biological molecules.<sup>1-10</sup> Interionic potentials of mean force

(PMF) can provide important insights into thermodynamics and kinetics of ion-ion interactions in solution. Calculations of PMF have been performed with integral equation techniques,<sup>3,5,6,9,10</sup> with the Langevin dipole model of solvent,<sup>1</sup> and with full microscopic simulations of the ion-ion interactions in water.<sup>4,6,8</sup> All these calculations yield two major minima in PMF for unlike ions: the solvent separated minimum and the contact minimum, with a barrier between them. It has been suggested that this shape of PMF is determined by a specific structure of water around the ion pairs and by saturation effects,<sup>3,5,9</sup> and thus can be predicted only by approaches that explicitly account for the molecularity of the solvent. RISM approach,<sup>3,5,6,9</sup> in particular, has been devised as a correction to the continuum theory at short ion-ion separations, at which continuum theory allegedly does not work. Results

- (1) Warshel, A.; Russell, S. T.; *Quart. Rev. Biophys.* **1984**, *17*, 283.
- (2) Computer Simulation of Chemical and Biochemical Systems. Beveridge, D. L.; Jorgensen, W. L., Eds.; *Ann. NY Acad. Sci.* **1986**, *482*.
- (3) Hirata, F.; Rossky, P. J.; Pettitt, B. M. *J. Chem. Phys.* **1983**, *78*, 4133.
- (4) Berkowitz, M.; Karim, O. A.; McCammon, J. A.; Rossky, P. J. *J. Chem. Phys.* **1984**, *105*, 577.
- (5) Pettitt, B. M.; Rossky, P. J. *J. Chem. Phys.* **1986**, *105*, 577.
- (6) Jorgensen, W. L.; Buckner, J. K.; Huston, S. E.; Rossky, P. J. *J. Am. Chem. Soc.* **1987**, *109*, 1891.
- (7) Klapper, I.; Hangstrom, R.; Fine, R.; Sharp, K.; Honig, B. *Proteins* **1986**, *1*, 47.
- (8) Dang, L. X.; Pettitt, B. M. *J. Am. Chem. Soc.* **1987**, *109*, 5531.

- (9) Hirata, F.; Levy, R. M. *J. Phys. Chem.* **1987**, *91*, 4788.
- (10) Levesque, D.; Weiss, J. J.; Patey, G. N. *J. Chem. Phys.* **1980**, *72*, 1887; Patey, G. N.; Carnie, S. L. *Ibid.* **1983**, *78*, 5183.